Acta Pharmaceutica Sinica B 2021;11(12):3847−3856

Chinese Pharmaceutical Association
Institute of Materia Medica, Chinese Academy of Medical Sciences

Acta Pharmaceutica Sinica B

www.elsevier.com/locate/apsb
www.sciencedirect.com

ORIGINAL ARTICLE

Bile acid homeostasis in female mice deficient in *Cyp7a1* and *Cyp27a1*

Daniel Rizzolo[a,b,d], Bo Kong[a], Rulaiha E. Taylor[a], Anita Brinker[b], Michael Goedken[c], Brian Buckley[a,b], Grace L. Guo[a,b,d,e,*]

[a]*Department of Pharmacology and Toxicology, School of Pharmacy, Rutgers University, Piscataway, NJ 08854, USA*
[b]*Environmental and Occupational Health Institute, Rutgers University, Piscataway, NJ 08854, USA*
[c]*Office of Research and Economic Development, Research Pathology Services, Rutgers University, Piscataway, NJ 08854, USA*
[d]*Rutgers Center of Lipid Research, Rutgers University, New Brunswick, NJ 08901, USA*
[e]*Department of Veterans Affairs New Jersey Health Care System, East Orange, NJ 07018, USA*

Received 28 December 2020; received in revised form 13 April 2021; accepted 13 May 2021

KEY WORDS

Bile acids;
Farnesoid X receptor;
Female;
Fibroblast growth factor 15;
CYP7A1;
CYP27A1

Abstract Bile acids (BAs) are amphipathic molecules important for metabolism of cholesterol, absorption of lipids and lipid soluble vitamins, bile flow, and regulation of gut microbiome. There are over 30 different BA species known to exist in humans and mice, which are endogenous modulators of at least 6 different membrane or nuclear receptors. This diversity of ligands and receptors play important roles in health and disease; however, the full functions of each individual BA *in vivo* remain unclear. We generated a mouse model lacking the initiating enzymes, CYP7A1 and CYP27A1, in the two main pathways of BA synthesis. Because females are more susceptible to BA related diseases, such as intrahepatic cholestasis of pregnancy, we expanded this model into female mice. The null mice of *Cyp7a1* and *Cyp27a1* were crossbred to create double knockout (DKO) mice. BA concentrations in female DKO mice had reductions in serum (63%), liver (83%), gallbladder (94%), and small intestine (85%), as compared to WT mice. Despite low BA levels, DKO mice had a similar expression pattern to that of WT mice for genes involved in BA regulation, synthesis, conjugation, and transport. Additionally, through treatment with a

Abbreviations: ALP, alkaline phosphatase; ALT, alanine aminotransferase; AST, aspartate transaminase; ASBT, apical sodium-dependent BA transporter; BA, bile acid; βMCA, beta muricholic acid; BSEP, bile salt export pump; CA, cholic acid; CDCA, chenodeoxycholic acid; CYP27A1, sterol 27-hydroxylase; CYP7A1, cholesterol 7α-hydroxylase; CYP7B1, 25-hydroxycholesterol 7-alpha-hydroxylase; CYP8B1, sterol 12α-hydroxylase; CYP2C70, cytochrome P450 2C70; DCA, deoxycholic acid; DKO, double knockout; FXR, farnesoid X receptor; IBABP, intestinal BA-binding protein; LCA, lithocholic acid; NTCP, sodium taurocholate cotransporting polypeptide; OSTα/β, organic solute transporters alpha and beta; OATP, organic anion transporters; WT, wild type.

*Corresponding author. Tel.: +1 848 4458186.
E-mail address: glg48@eohsi.rutgers.edu (Grace L. Guo).

Peer review under responsibility of Chinese Pharmaceutical Association and Institute of Materia Medica, Chinese Academy of Medical Sciences.

https://doi.org/10.1016/j.apsb.2021.05.023

synthetic FXR agonist, GW4064, female DKO mice responded to FXR activation similarly to WT mice.

1. Introduction

Bile acids (BAs) are amphipathic molecules synthesized through the enzymatic oxidation of cholesterol in the liver. BAs are generally conjugated to the amino acid glycine or taurine, which form negatively charged bile salts with increased solubility[1]. Following conjugation in hepatocytes, BAs are excreted into the bile canaliculi through the bile salt export pump (BSEP), where they are transported out of the liver and to the gallbladder for storage. Postprandial stimuli cause the gallbladder to contract, releasing BAs and pancreatic lipases into the duodenum. Inside the small intestine, BAs function as physiological detergents that aid in the digestion and absorption of dietary fats, cholesterol, and lipid soluble vitamins through the formation of mixed micelles. Most conjugated BAs are actively reabsorbed in the distal small intestine by the apical sodium-dependent BA transporter (ASBT)[2]. Deconjugated BAs can be passively reabsorbed in the large intestine. BAs reabsorbed in the ileum are shuttled across ileocytes by the intestinal BA-binding protein (IBABP) and effluxed into the portal circulation by heterodimer organic solute transporters alpha and beta (OSTα/β)[3]. Portal circulation carries reabsorbed BAs back to hepatocytes, where they are taken up by either sodium taurocholate cotransporting polypeptide (NTCP) or organic anion transporters (OATPs)[4,5]. Hepatocyte reabsorbed BAs can be detoxified through sulfoconjugation for excretion/elimination or recycled and reconjugated for reuse. BAs are reabsorbed at ~95% efficiency, with the excreted BA fraction being replaced by newly synthesized primary BAs[6]. The synthesis of new BAs from cholesterol represents the primary route of cholesterol removal from the body.

BA biosynthesis is predominantly driven by the classic (*i.e.*, neutral) and alternative (*i.e.*, acidic) pathways. The classic pathway is initiated by the rate-limiting enzyme, cholesterol 7α-hydroxylase (CYP7A1), which catalyzes the hydroxylation of cholesterol to 7α-hydroxycholesterol. The classic pathway produces the primary BAs cholic acid (CA) and chenodeoxycholic acid (CDCA) in roughly equal proportions. The differentiation between CA and CDCA formation is dependent upon 12α-hydroxylase (CYP8B1) activity, which performs an additional hydroxylation at the C_{12} position to produce CA[6]. The alternative pathway is initiated with the oxidation of the cholesterol side chain by the mitochondrial cytochrome P450 sterol 27-hydroxylase (CYP27A1). This is followed by the hydroxylation of C_7 by 25-hydroxycholesterol 7-alpha-hydroxylase (CYP7B1). In mice, the enzyme cytochrome P450 2C70 (CYP2C70) rapidly converts CDCA to β-muricholic acid (βMCA)[7]. Primary BAs are conjugated to either glycine or taurine before being transported to the gallbladder for storage. Following biliary excretion, conjugated primary BAs can be partially metabolized by intestinal microflora. Bacterial metabolism and hydroxylase activity can deconjugate primary BAs and convert them into more hydrophobic and cytotoxic secondary BAs, such as lithocholic acid (LCA) and deoxycholic acid (DCA)[8].

In addition to their role as physiological detergents, BAs have been shown to act as endocrine molecules that play roles in lipid and glucose homeostasis, energy expenditure, inflammation, liver and gastrointestinal functions, and gut bacterial proliferation. BAs accomplish these roles through interactions with both nuclear receptors and cell surface G protein-coupled receptors. The most well-known and well-studied BA receptor is the farnesoid X receptor (FXR), which acts as a master regulator for BA homeostasis through negative feedback regulation of BA synthesis and positive regulation of BA transport[9]. BAs have been found to activate other nuclear receptors including the pregnane X receptor[10,11] and the vitamin D receptor[12], both of which can induce CYP3A, potentially ameliorating the cytotoxic effects of lipophilic secondary BAs. Additionally, BAs can act as ligands for the membrane receptors Takeda G protein receptor 5[13,14], sphingosine-1-phosphate receptor 2[15], and cholinergic receptor muscarinic 2[16].

There are currently over 30 different BA species known to exist in humans and rodents[17,18]. The diversity of ligands and receptors play important roles in health and disease; however, the full functions of each individual BA *in vivo* remain unclear due to several model limitation: 1) the baseline diversity of BA species makes ascertaining the role of individual BAs difficult; 2) BA feeding is limited due to associated cytotoxicity; 3) BA feeding results in supraphysiological levels of BAs, which could affect the observed response. In order to overcome these limitations, we aimed to create a mouse model deficient in BAs that maintained the biological response to BA receptor activation. We have previously reported on the development of this model in male mice[19]. It is important to expand this model into female mice, as females are more susceptible to BA related diseases. In pregnancy for example, BA disregulation has been shown to increase the risk of preterm birth[20], and intrahepatic cholestasis of pregnancy, which can occur in over 5% of pregnancies[21,22], is characterized by elevated levels of serum BAs[23]. Furthermore, estrogen, which is more prevalent in females than males, is known to induce cholestasis and influence gallstone formation[24,25]. In the current study, we seek to characterize this model in female mice while exploring the potential for sex differences in BA biology.

2. Materials and methods

2.1. Experimental design

Cyp7a1$^{-/-}$ and *Cyp27a1*$^{-/-}$ double knockout (DKO) mice were developed as previously described[19]. In short, *Cyp7a1*$^{-/-}$ mice and *Cyp27a1*$^{-/-}$ mice were purchased from The Jackson Laboratory (Bar Harbor, ME, USA). The mice were crossbred to create *Cyp7a1*$^{-/+}$ and *Cyp27a1*$^{-/+}$ heterozygous F1 mice. F1 mice were crossed to create the DKO mice, deficient in both enzymes. Wild type (WT) mice from the F1 cross were used as liter mate controls. All genotyping was performed per The Jackson Laboratory protocols. To study the responsiveness of DKO mice to FXR activation, mice were treated with the synthetic FXR agonist GW4064. In detail, 3- to 4-month-old female mice were treated with either GW4064 (150 mg/kg) or vehicle control (1% Tween-

80 and 1% methylcellulose) at 6:00 pm, fasted overnight and received a second dose at 8:00 am, followed by euthanasia 2 h later. Blood was collected *via* retrobulbar bleeds. Liver, gallbladder, and intestines were collected during necropsy, flash frozen in liquid nitrogen, and stored at −80 °C for analysis. Vehicle treated control mice were used for BA profiling. All mice were group-housed in a temperature-controlled facility with 12-h light/dark cycles. Access to food and water was provided *ad libitum* unless noted otherwise. All experiments were performed under protocols approved by the Rutgers Institutional Animal Care and Use Committee. Additional animal information can be found in Supporting Information Table S1 and Fig. S1.

2.2. *Serum biochemistry*

Serum samples were analyzed for alanine aminotransferase (ALT), aspartate transaminase (AST), and alkaline phosphatase (ALP) activities as well as total cholesterol and triglyceride levels through the use of commercially available kits (Pointe Scientific, Canton, MI, USA).

2.3. *BA profiling*

The quantification and profiling of 22 unique BAs was performed as previously described[19]. BA extraction was performed from 90 µL of serum, ∼50 mg of liver tissue, whole gallbladder, and whole small intestine (including luminal content). An aliquot of suspended gallbladder content was diluted 50 × in PBS. A 300 µL aliquot of small intestine homogenate was used for analysis. All samples were subjected to acetonitrile protein precipitation. Samples were spun at 12,000×*g* for 10 min. The BA containing supernatant was dried under a speed-vac, reconstituted in 400 µL of 50% methanol, and passed through a 0.22 µm Costar Spin-X centrifuge tube. All purified, dried, and reconstituted samples were analyzed with a Thermo Accela Ultra Performance Chromatography system (Thermo Fisher Scientific, Waltham, MA, USA) using a reverse-phase 1.3 µm 2.1 mm × 50 mm C18 Kinetex column (Phenomenex, Torrance, CA, USA). The system was coupled to a Thermo Finnigan LTQ Ion Trap Mass Spectrometer (Thermo Fisher Scientific). The collected spectrometry data were analyzed using Xcalibur quantitation software version 2.0.3.

2.4. *Gene expression*

Total RNA extraction was performed on liver and ileum tissue with TRIzol reagent (Thermo Fisher Scientific). The extracted RNA was subjected to reverse transcription to attain complementary DNA. Real-time quantitative PCR with SYBR green chemistry was used on a ViiA7 Real Time PCR machine (Life Technologies, Grand Island, NY, USA) to determine relative gene expression. Samples were run on a 384-well plate (Life

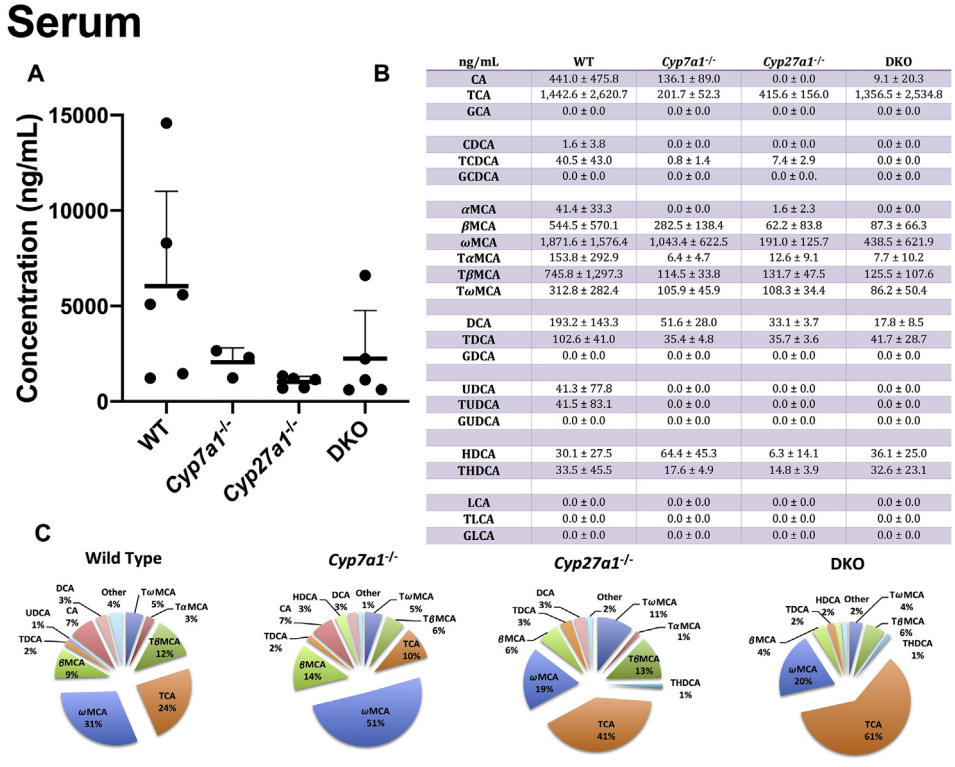

ng/mL	WT	*Cyp7a1*$^{-/-}$	*Cyp27a1*$^{-/-}$	DKO
CA	441.0 ± 475.8	136.1 ± 89.0	0.0 ± 0.0	9.1 ± 20.3
TCA	1,442.6 ± 2,620.7	201.7 ± 52.3	415.6 ± 156.0	1,356.5 ± 2,534.8
GCA	0.0 ± 0.0	0.0 ± 0.0	0.0 ± 0.0	0.0 ± 0.0
CDCA	1.6 ± 3.8	0.0 ± 0.0	0.0 ± 0.0	0.0 ± 0.0
TCDCA	40.5 ± 43.0	0.8 ± 1.4	7.4 ± 2.9	0.0 ± 0.0
GCDCA	0.0 ± 0.0	0.0 ± 0.0	0.0 ± 0.0.	0.0 ± 0.0
αMCA	41.4 ± 33.3	0.0 ± 0.0	1.6 ± 2.3	0.0 ± 0.0
βMCA	544.5 ± 570.1	282.5 ± 138.4	62.2 ± 83.8	87.3 ± 66.3
ωMCA	1,871.6 ± 1,576.4	1,043.4 ± 622.5	191.0 ± 125.7	438.5 ± 621.9
TαMCA	153.8 ± 292.9	6.4 ± 4.7	12.6 ± 9.1	7.7 ± 10.2
TβMCA	745.8 ± 1,297.3	114.5 ± 33.8	131.7 ± 47.5	125.5 ± 107.6
TωMCA	312.8 ± 282.4	105.9 ± 45.9	108.3 ± 34.4	86.2 ± 50.4
DCA	193.2 ± 143.3	51.6 ± 28.0	33.1 ± 3.7	17.8 ± 8.5
TDCA	102.6 ± 41.0	35.4 ± 4.8	35.7 ± 3.6	41.7 ± 28.7
GDCA	0.0 ± 0.0	0.0 ± 0.0	0.0 ± 0.0	0.0 ± 0.0
UDCA	41.3 ± 77.8	0.0 ± 0.0	0.0 ± 0.0	0.0 ± 0.0
TUDCA	41.5 ± 83.1	0.0 ± 0.0	0.0 ± 0.0	0.0 ± 0.0
GUDCA	0.0 ± 0.0	0.0 ± 0.0	0.0 ± 0.0	0.0 ± 0.0
HDCA	30.1 ± 27.5	64.4 ± 45.3	6.3 ± 14.1	36.1 ± 25.0
THDCA	33.5 ± 45.5	17.6 ± 4.9	14.8 ± 3.9	32.6 ± 23.1
LCA	0.0 ± 0.0	0.0 ± 0.0	0.0 ± 0.0	0.0 ± 0.0
TLCA	0.0 ± 0.0	0.0 ± 0.0	0.0 ± 0.0	0.0 ± 0.0
GLCA	0.0 ± 0.0	0.0 ± 0.0	0.0 ± 0.0	0.0 ± 0.0

Figure 1 Serum BA concentration and composition in female WT, *Cyp7a1*$^{-/-}$, *Cyp27a1*$^{-/-}$, and DKO mice. BAs were measured using UPLC−ITMS from 90 µL of serum. (A) Mean total BA concentration ± SD in the serum of female WT, *Cyp7a1*$^{-/-}$, *Cyp27a1*$^{-/-}$, and DKO mice displayed in ng/mL. (B) Mean concentration ± SD of 23 individual BAs. (C) Percent composition of BA species in serum. An asterisk signifies significant difference from WT mice ($P < 0.05$).

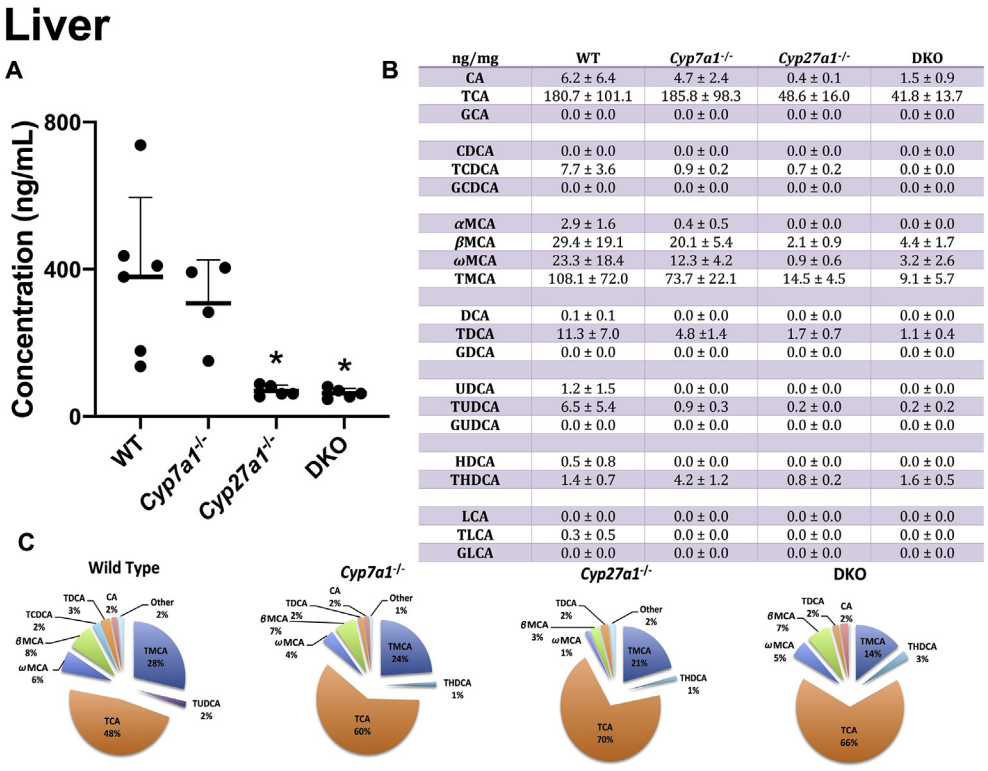

ng/mg	WT	*Cyp7a1*$^{-/-}$	*Cyp27a1*$^{-/-}$	DKO
CA	6.2 ± 6.4	4.7 ± 2.4	0.4 ± 0.1	1.5 ± 0.9
TCA	180.7 ± 101.1	185.8 ± 98.3	48.6 ± 16.0	41.8 ± 13.7
GCA	0.0 ± 0.0	0.0 ± 0.0	0.0 ± 0.0	0.0 ± 0.0
CDCA	0.0 ± 0.0	0.0 ± 0.0	0.0 ± 0.0	0.0 ± 0.0
TCDCA	7.7 ± 3.6	0.9 ± 0.2	0.7 ± 0.2	0.0 ± 0.0
GCDCA	0.0 ± 0.0	0.0 ± 0.0	0.0 ± 0.0	0.0 ± 0.0
αMCA	2.9 ± 1.6	0.4 ± 0.5	0.0 ± 0.0	0.0 ± 0.0
βMCA	29.4 ± 19.1	20.1 ± 5.4	2.1 ± 0.9	4.4 ± 1.7
ωMCA	23.3 ± 18.4	12.3 ± 4.2	0.9 ± 0.6	3.2 ± 2.6
TMCA	108.1 ± 72.0	73.7 ± 22.1	14.5 ± 4.5	9.1 ± 5.7
DCA	0.1 ± 0.1	0.0 ± 0.0	0.0 ± 0.0	0.0 ± 0.0
TDCA	11.3 ± 7.0	4.8 ±1.4	1.7 ± 0.7	1.1 ± 0.4
GDCA	0.0 ± 0.0	0.0 ± 0.0	0.0 ± 0.0	0.0 ± 0.0
UDCA	1.2 ± 1.5	0.0 ± 0.0	0.0 ± 0.0	0.0 ± 0.0
TUDCA	6.5 ± 5.4	0.9 ± 0.3	0.2 ± 0.0	0.2 ± 0.2
GUDCA	0.0 ± 0.0	0.0 ± 0.0	0.0 ± 0.0	0.0 ± 0.0
HDCA	0.5 ± 0.8	0.0 ± 0.0	0.0 ± 0.0	0.0 ± 0.0
THDCA	1.4 ± 0.7	4.2 ± 1.2	0.8 ± 0.2	1.6 ± 0.5
LCA	0.0 ± 0.0	0.0 ± 0.0	0.0 ± 0.0	0.0 ± 0.0
TLCA	0.3 ± 0.5	0.0 ± 0.0	0.0 ± 0.0	0.0 ± 0.0
GLCA	0.0 ± 0.0	0.0 ± 0.0	0.0 ± 0.0	0.0 ± 0.0

Figure 2 Liver BA concentration and composition in female WT, *Cyp7a1*$^{-/-}$, *Cyp27a1*$^{-/-}$, and DKO mice. BAs were measured using UPLC−ITMS from ∼50 mg of liver tissue. (A) Mean total BA concentration ± SD in the liver of female WT, *Cyp7a1*$^{-/-}$, *Cyp27a1*$^{-/-}$, and DKO mice displayed as ng of BA/mg liver tissue. (B) Mean concentration ± SD of 21 individual BAs. (C) Percent composition of BA species in liver tissue. An asterisk signifies significant difference from WT mice ($P < 0.05$).

Technologies). All CT values were normalized to β-actin mRNA levels and converted to delta delta CT values. All primer sequences used in this study are provided in Supporting Information Table S2.

2.5. *Histology*

Liver samples collected during necropsy were fixed in 10% PBS neutral buffered formalin and embedded in paraffin wax. 5 μm sections of liver tissue were stained using hematoxylin and eosin (H&E).

2.6. *Statistical analysis*

Groups were compared using a one-way ANOVA and Tukey's *post hoc* test unless otherwise noted. For the GW4064 study, groups were compared using a two-way ANOVA and Tukey's *post hoc* test. Data are displayed as mean ± standard deviation (SD, $n = 4–6$). All data were analyzed using SAS Studio software (2020 SAS Institute Inc.). Significance was considered at $P < 0.05$.

3. Results

3.1. *Serum lipids, markers of liver injury, and histology*

Serum activities of ALT, AST, and ALP were measured as markers of liver injury. There was no significant difference between WT and any of the KO groups. Additionally, we measured serum triglyceride and total cholesterol levels and found no significant difference among these 4 groups (Supporting Information Fig. S2). H&E-stained liver sections were examined by a board-certified pathologist and no significant difference among these 4 groups was observed (Supporting Information Fig. S3). Taken together, these data suggest that knocking out *Cyp7a1* and/or *Cyp27a1* did not induce liver injury in our model.

3.2. *The impact of Cyp7a1 and Cyp27a1 deficiencies on BA levels, profile, and disposition*

3.2.1. *Serum BAs*

Serum BA profiling was performed in 3−4-month-old female WT, *Cyp7a1*$^{-/-}$, *Cyp27a1*$^{-/-}$, and DKO mice (Fig. 1). WT mice had a total serum concentration of 6037 ± 4965 ng/mL. *Cyp7a1*$^{-/-}$, *Cyp27a1*$^{-/-}$, and DKO mice had reductions in total serum BAs of 66%, 83%, and 63% respectively. In WT mice, 52% of BAs were unconjugated, with the most prevalent BAs being ωMCA (31%), TCA (24%) and T-βMCA (12%). *Cyp7a1*$^{-/-}$ mice had an average BA serum concentration of 2060 ± 743 ng/mL. Secondary BAs represented 71% of serum BAs in *Cyp7a1*$^{-/-}$, with ωMCA (51%) being most abundant. In *Cyp27a1*$^{-/-}$ mice, 71% of BAs were tauro-conjugated BAs, which largely consisted of TCA (41%) and T-βMCA (13%). DKO mice had a serum concentration of 2239 ± 2532 ng/mL, a reduction of 63% as compared to WT mice. The most abundant BAs in the serum of DKO mice were TCA (61%), ωMCA (20%), T-βMCA (6%), and βMCA (4%). A complete table of the average concentrations of the 23 serum BAs measured can be found in Fig. 1B.

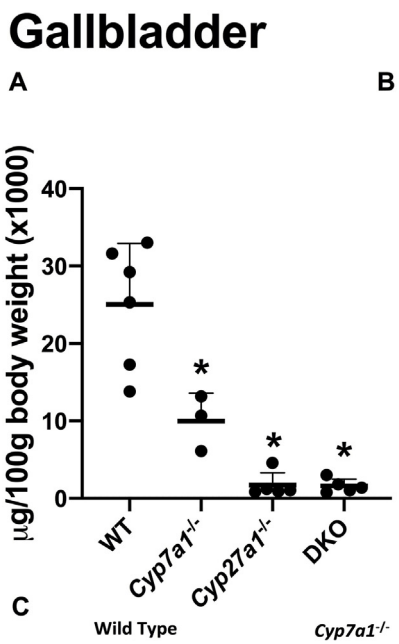

	WT	*Cyp7a1*$^{-/-}$	*Cyp27a1*$^{-/-}$	DKO
CA	0.1 ± 0.2	0.0 ± 0.0	0.0 ± 0.0	0.0 ± 0.0
TCA	12.9 ± 5.4	5.5 ± 3.2	0.9 ± 1.3	0.8 ± 0.6
GCA	0.0 ± 0.0	0.0 ± 0.0	0.0 ± 0.0	0.0 ± 0.0
CDCA	0.0 ± 0.0	0.0 ± 0.0	0.0 ± 0.0	0.0 ± 0.0
TCDCA	0.4 ± 0.2	0.0 ± 0.0	0.0 ± 0.0	0.0 ± 0.0
GCDCA	0.0 ± 0.0	0.0 ± 0.0	0.0 ± 0.0	0.0 ± 0.0
αMCA	0.0 ± 0.0	0.0 ± 0.0	0.0 ± 0.0	0.0 ± 0.0
βMCA	0.1 ± 0.1	0.0 ± 0.0	0.0 ± 0.0	0.0 ± 0.0
ωMCA	0.2 ± 0.3	0.0 ± 0.0	0.0 ± 0.0	0.0 ± 0.0
TαMCA	1.0 ± 0.4	0.3 ± 0.1	0.2 ± 0.0	0.2 ± 0.0
TβMCA	5.9 ± 1.6	2.2 ± 0.6	0.4 ± 0.2	0.4 ± 0.2
TωMCA	3.1 ± 1.7	1.6 ± 0.6	0.2 ± 0.1	0.2 ± 0.1
DCA	0.0 ± 0.0	0.0 ± 0.0	0.0 ± 0.0	0.0 ± 0.0
TDCA	0.7 ± 0.4	0.1 ± 0.1	0.0 ± 0.0	0.0 ± 0.0
GDCA	0.0 ± 0.0	0.0 ± 0.0	0.0 ± 0.0	0.0 ± 0.0
UDCA	0.0 ± 0.0	0.0 ± 0.0	0.0 ± 0.0	0.0 ± 0.0
TUDCA	0.5 ± 0.2	0.0 ± 0.0	0.0 ± 0.0	0.0 ± 0.0
GUDCA	0.0 ± 0.0	0.0 ± 0.0	0.0 ± 0.0	0.0 ± 0.0
HDCA	0.0 ± 0.0	0.0 ± 0.0	0.0 ± 0.0	0.0 ± 0.0
THDCA	0.2 ± 0.1	0.2 ± 0.1	0.0 ± 0.0	0.0 ± 0.0
LCA	0.0 ± 0.0	0.0 ± 0.0	0.0 ± 0.0	0.0 ± 0.0
TLCA	0.0 ± 0.0	0.0 ± 0.0	0.0 ± 0.0	0.0 ± 0.0
GLCA	0.0 ± 0.0	0.0 ± 0.0	0.0 ± 0.0	0.0 ± 0.0

Figure 3 Gallbladder BA concentration and composition in female WT, *Cyp7a1*$^{-/-}$, *Cyp27a1*$^{-/-}$, and DKO mice. BAs were measured using UPLC−ITMS from gallbladder content. (A) Mean total BA concentration ± SD in the gallbladder of female WT, *Cyp7a1*$^{-/-}$, *Cyp27a1*$^{-/-}$, and DKO mice displayed as μg of BA/100 g body weight (× 1000). (B) Mean concentration ± SD of 23 individual BAs. (C) Percent composition of BA species in the gallbladder. An asterisk signifies significant difference from WT mice ($P < 0.05$).

3.2.2. *Liver BAs*

In the liver of WT mice (Fig. 2), the average BA concentration was 380 ± 215 ng/mg of liver tissue. The majority of BAs in the liver were taurine conjugated primary BAs, regardless of genotype. The most prevalent hepatic BAs in WT mice were TCA (48%), T-MCA (28%), and βMCA (8%). *Cyp7a1*$^{-/-}$ mice had a 19% reduction in hepatic BAs, with an average concentration of 308 ± 118 ng/mg liver tissue. *Cyp27a1*$^{-/-}$ mice had a significant reduction of 82%, as compared to WT mice. The most abundant hepatic BAs in *Cyp27a1*$^{-/-}$ mice were TCA (70%), T-MCA (21%), and βMCA (3%). DKO mice had a significant reduction of 83% in liver BA concentration. The average concentration of hepatic BAs in DKO mice was 63 ± 13 ng/mg liver tissue, with TCA (66%), T-MCA (14%) and βMCA (7%) being most abundant.

3.2.3. *Gallbladder BAs*

BAs are synthesized or recycled in liver and conjugated to either taurine or glycine before being stored in the gallbladder for use. Profiling (Fig. 3) showed that over 98% of BAs were conjugated in the gallbladder of WT mice, and were conjugated 99%, 100%, and 100% in *Cyp7a1*$^{-/-}$, *Cyp27a1*$^{-/-}$, and DKO mice, respectively. WT mice had an average gallbladder BA concentration of 25 ± 8 mg/100 g body weight. The most enriched BAs in the gallbladder of WT mice were TCA (51%), T-βMCA (24%), and T-ωMCA (12%). *Cyp7a1*$^{-/-}$ mice had a significant reduction of gallbladder BAs of 60%, with the most abundant BAs being TCA (55%), T-βMCA (22%), and T-ωMCA (16%). *Cyp27a1*$^{-/-}$ mice had a 93% reduction in gallbladder BA concentration as compared to WT, which consisted largely of TCA (54%), T-βMCA (22%), and T-αMCA (14%). DKO mice had a significant 94% reduction in gallbladder BA concentration as compared to WT mice, with 100% of BAs being conjugated and 84% being the primary BAs TCA (48%), T-βMCA (24%), and T-αMCA (12%).

3.2.4. *Small intestine BAs*

The small intestine contains roughly 70% of the total BA pool. WT mice had an average small intestine BA concentration of 53 ± 12 mg/100 g body weight. *Cyp7a1*$^{-/-}$ mice had a significant 75% reduction of small intestine BAs, predominantly consisting of CA (36%), ωMCA (31%), and βMCA (18%). *Cyp27a1*$^{-/-}$ mice had a 79% reduction of small intestine BAs, with an average concentration of 11 ± 5 mg/100 g body weight. The majority of small intestine BAs in *Cyp27a1*$^{-/-}$ mice were the conjugated primary BAs TCA (51%) and TMCA (21%). DKO mice had a significant reduction of small intestine BAs of 85%, with a mean concentration of 8 ± 5 mg/100 g body weight. The most abundant

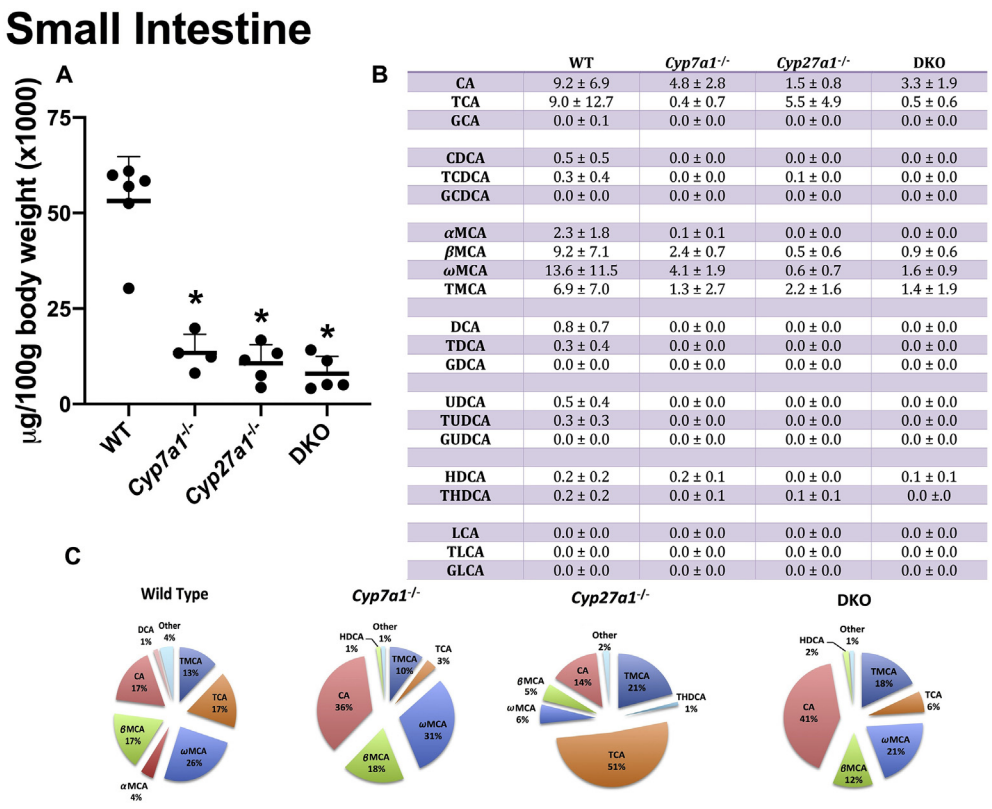

	WT	*Cyp7a1*$^{-/-}$	*Cyp27a1*$^{-/-}$	DKO
CA	9.2 ± 6.9	4.8 ± 2.8	1.5 ± 0.8	3.3 ± 1.9
TCA	9.0 ± 12.7	0.4 ± 0.7	5.5 ± 4.9	0.5 ± 0.6
GCA	0.0 ± 0.1	0.0 ± 0.0	0.0 ± 0.0	0.0 ± 0.0
CDCA	0.5 ± 0.5	0.0 ± 0.0	0.0 ± 0.0	0.0 ± 0.0
TCDCA	0.3 ± 0.4	0.0 ± 0.0	0.1 ± 0.0	0.0 ± 0.0
GCDCA	0.0 ± 0.0	0.0 ± 0.0	0.0 ± 0.0	0.0 ± 0.0
αMCA	2.3 ± 1.8	0.1 ± 0.1	0.0 ± 0.0	0.0 ± 0.0
βMCA	9.2 ± 7.1	2.4 ± 0.7	0.5 ± 0.6	0.9 ± 0.6
ωMCA	13.6 ± 11.5	4.1 ± 1.9	0.6 ± 0.7	1.6 ± 0.9
TMCA	6.9 ± 7.0	1.3 ± 2.7	2.2 ± 1.6	1.4 ± 1.9
DCA	0.8 ± 0.7	0.0 ± 0.0	0.0 ± 0.0	0.0 ± 0.0
TDCA	0.3 ± 0.4	0.0 ± 0.0	0.0 ± 0.0	0.0 ± 0.0
GDCA	0.0 ± 0.0	0.0 ± 0.0	0.0 ± 0.0	0.0 ± 0.0
UDCA	0.5 ± 0.4	0.0 ± 0.0	0.0 ± 0.0	0.0 ± 0.0
TUDCA	0.3 ± 0.3	0.0 ± 0.0	0.0 ± 0.0	0.0 ± 0.0
GUDCA	0.0 ± 0.0	0.0 ± 0.0	0.0 ± 0.0	0.0 ± 0.0
HDCA	0.2 ± 0.2	0.2 ± 0.1	0.0 ± 0.0	0.1 ± 0.1
THDCA	0.2 ± 0.2	0.0 ± 0.1	0.1 ± 0.1	0.0 ±.0
LCA	0.0 ± 0.0	0.0 ± 0.0	0.0 ± 0.0	0.0 ± 0.0
TLCA	0.0 ± 0.0	0.0 ± 0.0	0.0 ± 0.0	0.0 ± 0.0
GLCA	0.0 ± 0.0	0.0 ± 0.0	0.0 ± 0.0	0.0 ± 0.0

Figure 4 Small intestine BA concentration and composition in female WT, *Cyp7a1*$^{-/-}$, *Cyp27a1*$^{-/-}$, and DKO mice. BAs were measured using UPLC−ITMS from homogenized small intestine. (A) Mean total BA concentration ± SD in the small intestine of female WT, *Cyp7a1*$^{-/-}$, *Cyp27a1*$^{-/-}$, and DKO mice displayed as μg of BA/100 g body weight (× 1000). (B) Mean concentration ± SD of 21 individual BAs. (C) Percent composition of BA species in the small intestine. An asterisk signifies significant difference from WT mice ($P < 0.05$).

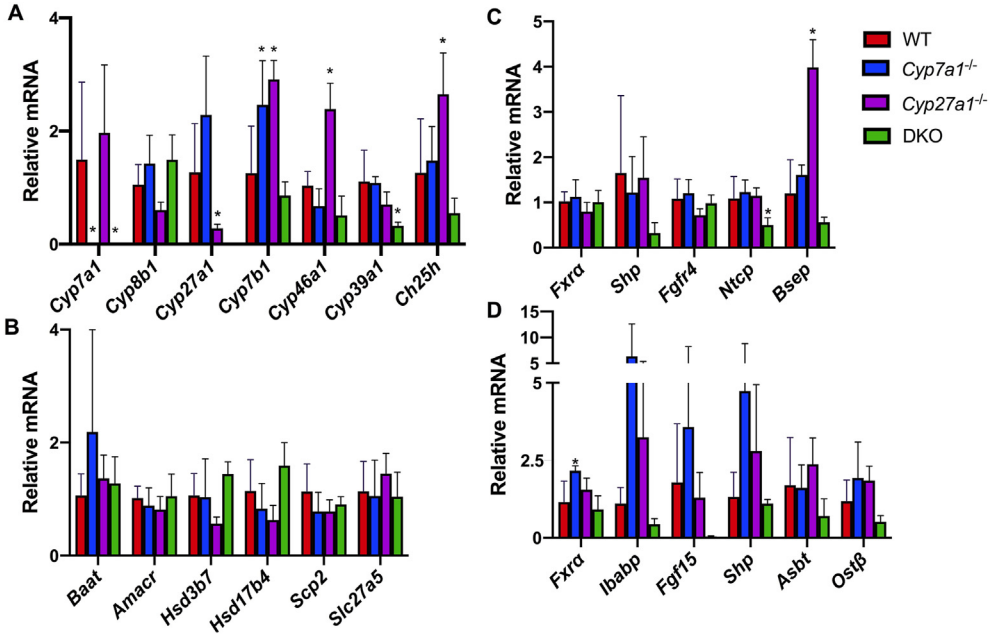

Figure 5 Relative mRNA expression of BA synthesis, regulation, and transport genes. Gene expression at mRNA levels was measured by RT-qPCR and normalized to β-actin mRNA expression. All graphs display relative mRNA levels ± SD. An asterisk signifies significant difference from WT mice ($P < 0.05$). Hepatic relative mRNA expression of genes involved in BA synthesis (A), synthesis and conjugation (B), regulation and transport (C). (D) Ileal relative mRNA expression of genes involved in BA regulation and transport.

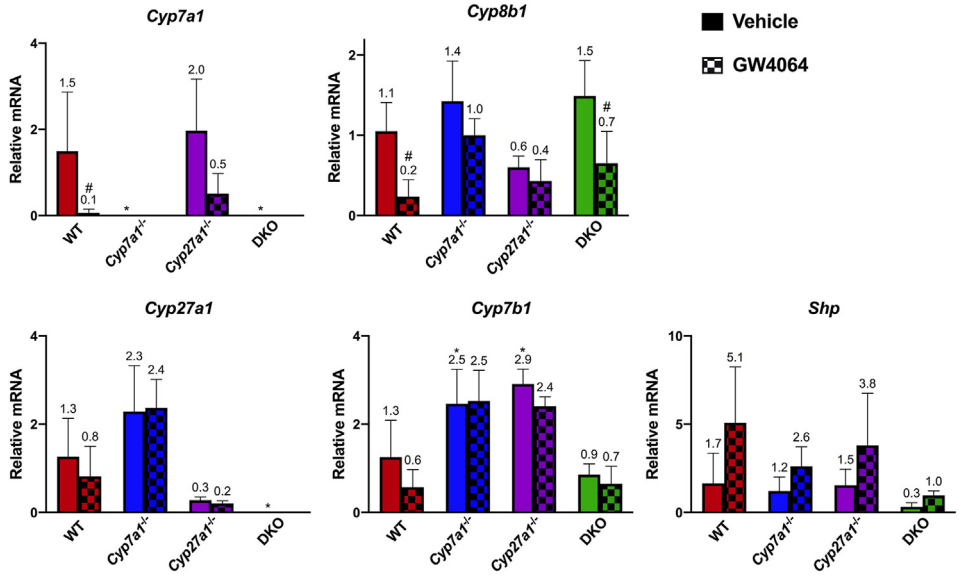

Figure 6 Hepatic relative mRNA expression following treatment with a synthetic FXR agonist, GW4064. Gene expression at mRNA levels was measured by RT-qPCR and normalized to β-actin mRNA expression. All graphs display relative mRNA expression $\pm$ SD. An asterisk signifies significant difference from vehicle-treated WT mice and a pound sign signifies a significant difference within genotypes between vehicle and GW4064 treatments ($P < 0.05$).

small intestine BAs in DKO mice were CA (41%), ωMCA (21%), and TMCA (18%) (Fig. 4).

3.3. *Expression of genes in BA regulation, synthesis, and transport*

3.3.1. *Hepatic expression of genes in BA regulation, synthesis, and transport*

The hepatic expression for 13 genes involved in BA synthesis and conjugation (*Cyp7a1*, *Cyp8b1*, *Cyp27a1*, *Cyp7b1*, *Cyp46a1*, *Cyp39a1*, *Ch25h*, *Baat*, *Amacr*, *Hsd3b7*, *Hsd17b4*, *Scp2*, and *Slc27a5*) are shown in Fig. 5. In Fig. 5A, the mRNA expression of *Cyp7a1* that encodes the rate limiting enzyme in the classical pathway of BA synthesis was below our level of detection in its corresponding knockout groups, *Cyp7a1*$^{-/-}$ and DKO. *Cyp27a1*, which encodes the initial enzyme in the alternative pathway of BA synthesis, had an expression below our level of detection in DKO mice. The expression of *Cyp8b1*, which is critical for the CA to CDCA (or MCA in mice) ratio *via* a 12-alpha hydroxylation, was not significantly altered in any knockout group. *Cyp46a1 and Ch25h*, which initiate the 24-hydroxylase and 25-hydroxylase minor pathways of BA synthesis, both displayed a significant increase of mRNA expression in *Cyp27a1*$^{-/-}$ mice with no significant alterations observed in the *Cyp7a1*$^{-/-}$ or DKO mice. Fig. 5B shows the expression of genes involved in intermediate BA synthesis, conjugation, and side chain cleavage. There were no significant changes of the mRNA expression of *Baat*, *Amacr*, *Hsd3b7*, *Hsd17b4*, *Scp2*, or *Slc27a5* between WT and other groups. The expression of 6 hepatic genes (*Fxrα*, *Fxrβ*, *Shp*, *Fgfr4*, *Ntcp*, and *Bsep*) involved in BA regulation and transport are shown in Fig. 5C. *Fxrα*, *Fxrβ* and an FXR target gene in BA regulation, *Shp*, showed no significant changes in gene expression between groups. *Ntcp*, which is responsible for the sinusoidal uptake of conjugated BAs showed no significant difference at the mRNA level between WT and *Cyp7a1*$^{-/-}$ or *Cyp27a1*$^{-/-}$. DKO mice had a significant 53.6% reduction in *Ntcp* gene expression as compared to WT mice. *Bsep*, a canalicular BA efflux transporter, showed no change in expression between WT, *Cyp7a1*$^{-/-}$, and DKO mice. *Cyp27a1*$^{-/-}$ mice had a significant 3.3-fold increase in *Bsep* mRNA expression as compared to WT. The ileal gene expression of 6 genes (*Fxrα*, *Ibabp*, *Fgf15*, *Shp*, *Asbt*, and *Ostβ)* involved in BA transport and regulation are shown in Fig. 5D. *Cyp7a1*$^{-/-}$ mice had a significant 1.87-fold induction of *Fxrα* mRNA expression as compared to WT mice, with no significant alterations observed in *Cyp27a1*$^{-/-}$ or DKO mice. *Ibabp*, *Fgf15*, *Shp*, *Asbt*, and *Ostβ* are ileal FXR target genes involved in BA transport and regulation. While there were variations observed in the ileal mRNA expression of these genes, there were no significant differences found in *Cyp7a1*$^{-/-}$, *Cyp27a1*$^{-/-}$, or DKO mice as compared to WT mice. The mRNA levels of Fxrβ were undetectable.

3.4. *FXR responsiveness to activation by synthetic agonist GW4064*

In order to study the roles of individual BA species, our model must respond to interactions between BAs and their receptors. FXR is a BA-activated nuclear receptor with well-studied target gene response following activation. To determine the responsiveness of FXR to agonists in DKO mice, we treated mice with vehicle control or GW4064, a synthetic FXR agonist, and measured relative gene expression in the liver and ileum. *Cyp7a1* is known to be negatively regulated following FXR activation. In WT mice (Fig. 6), GW4064 treatment significantly reduced hepatic *Cyp7a1* expression. *Cyp7a1*$^{-/-}$ and DKO mice did not express *Cyp7a1* and therefore displayed no response; *Cyp27a1*$^{-/-}$ had a 74.2% reduction in *Cyp7a1* mRNA expression. *Cyp8b1* expression is also suppressed following FXR activation. WT and DKO mice had significant reductions in *Cyp8b1* expression of 78% and 55%, respectively, following GW4064 treatment. SHP,

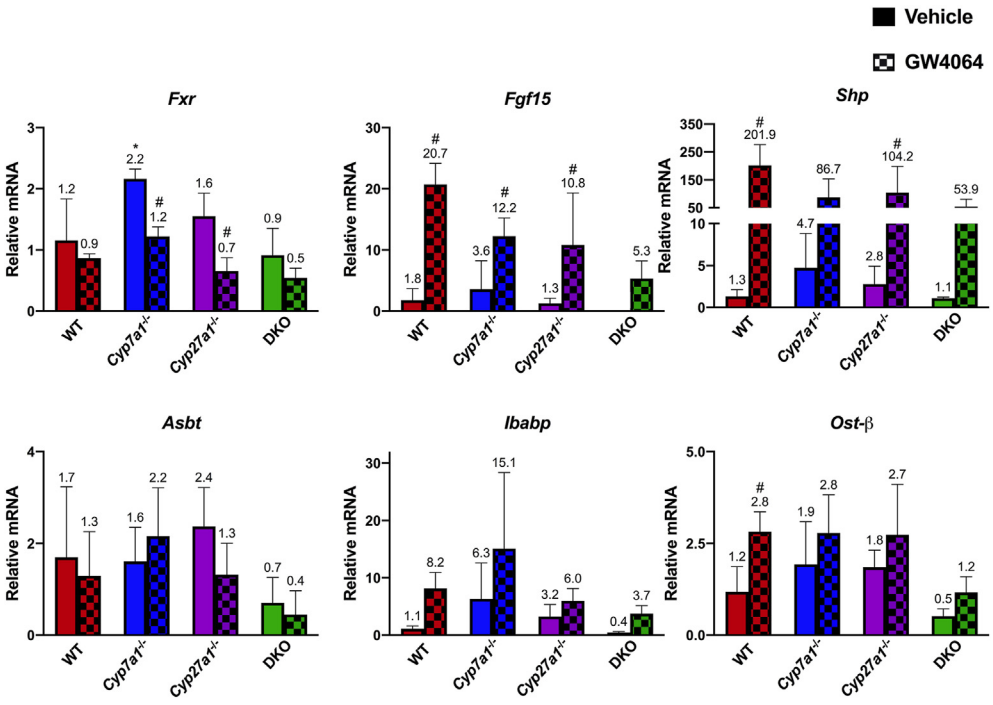

Figure 7 Ileal relative mRNA expression following treatment with a synthetic FXR agonist, GW4064. Gene expression at mRNA levels was measured by RT-qPCR and normalized to β-actin mRNA expression. All graphs display relative mRNA values $\pm$ SD. An asterisk signifies significant difference from vehicle-treated WT mice and a pound sign signifies a significant difference within genotypes between vehicle and GW4064 treatments ($P < 0.05$).

an orphan nuclear receptor involved in suppressing *Cyp7a1* transcription, is induced by FXR activation. All groups displayed greater than a 2-fold induction in *Shp* mRNA expression following GW4064 treatment, as compared to their vehicle treated counterparts. *Cyp27a1* and *Cyp7b1* expression is not regulated by FXR. In agreement with this, we see no significant change between vehicle and GW4064 treated mice in the mRNA expression of *Cyp27a1* or *Cyp7b1* in any group.

The mRNA expression of ileal genes following GW4064 treatment is displayed in Fig. 7. Treatment with GW4064 did not significantly alter the expression of *Fxr* or *Asbt* in WT or DKO mice. FGF15 is produced in the ileum and acts as an endocrine molecule that suppresses hepatic BA synthesis. *Fgf15* expression is known to be strongly induced by ileal FXR activation. All groups responded to GW4064 treatment by inducing the mRNA levels of *Fgf15*. *Shp* expression is also positively regulated following FXR activation. All groups had an over 50-fold induction of *Shp* mRNA expression in response to GW4064. OSTβ aids in basolateral BA efflux and is positively regulated by FXR. WT mice displayed a significant increase in *Ostβ* expression, while knockout groups that had higher basal levels showed a trend for induction with DKO mice being induced 2.25-fold as compared to DKO vehicle treated mice. *Ibabp*, which is positively regulated by FXR activation showed robust increases in all GW4064 treated groups, but failed to reach significance due to large variation.

4. Discussion

There are currently a multitude of FDA approved therapies that exploit aspects of FXR and BA signaling, including the use of individual BA, such as ursodeoxycholic acid (UDCA) for the treatment of primary biliary cholangitis or CDCA replacement therapy for the treatment of cerebrotendinous xanthomatosis, a human genetic diseases due to *CYP27A1* mutation. In addition to currently approved therapies, pharmaceutical companies continue to probe these pathways for the potential of disease intervention, such as the prospective use of FXR agonists for the treatment of nonalcoholic steatohepatitis (NASH). Improved understanding of BA biology and signaling through their interactions with nuclear and membrane bound receptors has the ability to provide new targets for drug therapy and to enhance our understanding of the role of BAs in many disease pathologies.

In the present study, we characterized the BA profile, hepatic/ileal gene expression, and the responsiveness to FXR activation in female mice deficient in *Cyp7a1* and/or *Cyp27a1*. We found that our DKO mice had reductions of total BAs of 63%, 83%, 94%, and 85% in the serum, liver, gallbladder, and small intestine, respectively, as compared to WT mice. When compared to the male mice in our previous study[19], WT and DKO mice had increased basal BA levels, which is in line with known sex differences. Aside from the intentional knockout of *Cyp7a1* and *Cyp27a1*, female DKO had either a reduction or no significant change in the expression of key genes measure in BA synthesis (*Cyp8b1*, *Cyp7b1*, *Cyp46a1*, *Cyp39a1*, *Ch25h*, *Baat*, *Amacr*, *Hsd3b7*, *Hsd17b4*, *Scp2*, and *Slc27a5*), transport (*Ntcp*, *Bsep*, *Ibabp*, *Asbt*, and *Ostβ*), and regulation (*Fxrα*, *Shp*, and *Fgf15*).

In order to determine if there was any alteration in the responsiveness of DKO mice to FXR agonism, we treated WT, *Cyp7a1*$^{-/-}$, *Cyp27a1*$^{-/-}$, and DKO mice with GW4064, a synthetic FXR agonist. Significant reductions in the hepatic expression of *Cyp7a1* and *Cyp8b1*, as well as significant induction in the ileal expression of *Fgf15* and *Shp* in WT mice indicate the treatment was effective in activating FXR. The female DKO mice

mirrored WT mice with a significant reduction in the hepatic expression of *Cyp8b1*, while *Cyp7a1*$^{-/-}$ and *Cyp27a1*$^{-/-}$ single knockout groups displayed non-significant reductions in the expression of *Cyp8b1* following GW4064 treatment. In the ileum, all groups responded similarly to WT mice following GW4064 treatment with robust mRNA inductions of FXR target genes *Fgf15* and *Shp*. These results suggest that WT and DKO mice respond similarly to FXR agonism. This piece of data also suggests that despite lower BA levels during development, FXR function and expression in liver and intestine remain unaltered. DKO mice appear healthy and there are no observed abnormalities during development. The low levels of bile acids will make these mice more susceptible to poor lipid and lipid soluble vitamin absorption. We anticipate these mice will accumulate less body fat and may be more insulin sensitive on a high-fat diet. These mice may serve as a model to study individual BAs or other FXR signaling modulators, as well as the potential for interactions with FXR in the liver and the intestine.

5. Conclusions

In this and our past study, we characterized a novel mouse model with dual deficiency in major BA synthetic enzymes. The DKO mice have no observed abnormalities during development, despite low BA levels. This model may be used to elucidate the role of individual BA species or FXR modulator *in vivo*, without the influence of endogenous, abundant and diverse BA species. Cross-breeding mice lacking the initial enzyme in each of the two main pathways of BA synthesis resulted in female DKO mice that had a total BA pool reduction of >85%. The DKO mice had a similar mRNA expression pattern to WT mice for key genes involved in BA synthesis, transport, and regulation. Additionally, female DKO mice responded to FXR activation in a similar manner to WT mice.

Acknowledgments

This work was supported by the National Institutes of Health (NIH-R01GM104037; NIH-R21ES029258; NIH-T32ES007148;VA-BX0 02741;NIH-F31DK122725; RCLR graduate student award fund, USA). Graphical abstract created with BioRender.com.

Author contributions

Daniel Rizzolo performed animal work, designed/performed experiments and prepared the manuscript. Bo Kong performed animal work and experiments. Rulaiha E. Taylor, Anita Brinker, and Brian Buckley performed analytical experiments and analysis. Michael Goedken evaluated histology. Grace L. Guo designed the research and revised the manuscript. All authors have read and approved the final manuscript.

Conflicts of interest

The authors of this study have no conflict of interest.

Appendix A. Supporting information

Supporting data to this article can be found online at https://doi.org/10.1016/j.apsb.2021.05.023.

References

1. Li T, Chiang JY. Bile acid signaling in metabolic disease and drug therapy. *Pharmacol Rev* 2014;**66**:948–83.
2. Wong MH, Oelkers P, Craddock AL, Dawson PA. Expression cloning and characterization of the hamster ileal sodium-dependent bile acid transporter. *J Biol Chem* 1994;**269**:1340–7.
3. Dawson PA, Hubbert M, Haywood J, Craddock AL, Zerangue N, Christian WV, et al. The heteromeric organic solute transporter alpha-beta, Ostalpha-Ostbeta, is an ileal basolateral bile acid transporter. *J Biol Chem* 2005;**280**:6960–8.
4. Hagenbuch B, Meier PJ. Molecular cloning, chromosomal localization, and functional characterization of a human liver Na^+/bile acid cotransporter. *J Clin Invest* 1994;**93**:1326–31.
5. Jacquemin E, Hagenbuch B, Stieger B, Wolkoff AW, Meier PJ. Expression cloning of a rat liver Na^+-independent organic anion transporter. *Proc Natl Acad Sci U S A* 1994;**91**:133–7.
6. Chiang JY. Bile acid metabolism and signaling. *Comp Physiol* 2013;**3**:1191–212.
7. Takahashi S, Fukami T, Masuo Y, Brocker CN, Xie C, Krausz KW, et al. Cyp2c70 is responsible for the species difference in bile acid metabolism between mice and humans. *J Lipid Res* 2016;**57**:2130–7.
8. Ridlon JM, Kang DJ, Hylemon PB, Bajaj JS. Bile acids and the gut microbiome. *Curr Opin Gastroenterol* 2014;**30**:332–8.
9. Makishima M, Okamoto AY, Repa JJ, Tu H, Learned RM, Luk A, et al. Identification of a nuclear receptor for bile acids. *Science* 1999;**284**:1362.
10. Staudinger JL, Goodwin B, Jones SA, Hawkins-Brown D, MacKenzie KI, LaTour A, et al. The nuclear receptor PXR is a lithocholic acid sensor that protects against liver toxicity. *Proc Natl Acad Sci U S A* 2001;**98**:3369–74.
11. Xie W, Radominska-Pandya A, Shi Y, Simon CM, Nelson MC, Ong ES, et al. An essential role for nuclear receptors SXR/PXR in detoxification of cholestatic bile acids. *Proc Natl Acad Sci U S A* 2001;**98**:3375–80.
12. Makishima M, Lu TT, Xie W, Whitfield GK, Domoto H, Evans RM, et al. Vitamin D receptor as an intestinal bile acid sensor. *Science* 2002;**296**:1313–6.
13. Kawamata Y, Fujii R, Hosoya M, Harada M, Yoshida H, Miwa M, et al. A G protein-coupled receptor responsive to bile acids. *J Biol Chem* 2003;**278**:9435–40.
14. Maruyama T, Miyamoto Y, Nakamura T, Tamai Y, Okada H, Sugiyama E, et al. Identification of membrane-type receptor for bile acids (M-BAR). *Biochem Biophys Res Commun* 2002;**298**:714–9.
15. Studer E, Zhou X, Zhao R, Wang Y, Takabe K, Nagahashi M, et al. Conjugated bile acids activate the sphingosine-1-phosphate receptor 2 in primary rodent hepatocytes. *Hepatology (Baltimore)* 2012;**55**:267–76.
16. Sheikh Abdul Kadir SH, Miragoli M, Abu-Hayyeh S, Moshkov AV, Xie Q, Keitel V, et al. Bile acid-induced arrhythmia is mediated by muscarinic M2 receptors in neonatal rat cardiomyocytes. *PLoS One* 2010;**5**:e9689.
17. Hofmann AF. Bile acids: trying to understand their chemistry and biology with the hope of helping patients. *Hepatology (Baltimore)* 2009;**49**:1403–18.
18. Han J, Liu Y, Wang R, Yang J, Ling V, Borchers CH. Metabolic profiling of bile acids in human and mouse blood by LC–MS/MS in combination with phospholipid-depletion solid-phase extraction. *Anal Chem* 2015;**87**:1127–36.
19. Rizzolo D, Buckley K, Kong B, Zhan L, Shen J, Stofan M, et al. Bile acid homeostasis in a cholesterol 7α-hydroxylase and sterol 27-hydroxylase double knockout mouse model. *Hepatology (Baltimore)* 2019;**70**:389–402.
20. You S, Cui AM, Hashmi SF, Zhang X, Nadolny C, Chen Y, et al. Dysregulation of bile acids increases the risk for preterm birth in pregnant women. *Nat Commun* 2020;**11**:2111.

21. Lee RH, Goodwin TM, Greenspoon J, Incerpi M. The prevalence of intrahepatic cholestasis of pregnancy in a primarily Latina Los Angeles population. *J Perinatol* 2006;**26**:527–32.
22. Floreani A, Gervasi MT. New insights on intrahepatic cholestasis of pregnancy. *Clin Liver Dis* 2016;**20**:177–89.
23. Pusl T, Beuers U. Intrahepatic cholestasis of pregnancy. *Orphanet J Rare Dis* 2007;**2**:26.
24. Chen J, Zhao KN, Liu GB. Estrogen-induced cholestasis: pathogenesis and therapeutic implications. *Hepatogastroenterology* 2013;**60**:1289–96.
25. Everson GT, McKinley C, Kern Jr F. Mechanisms of gallstone formation in women. Effects of exogenous estrogen (Premarin) and dietary cholesterol on hepatic lipid metabolism. *J Clin Invest* 1991;**87**:237–46.